

***Geomechanical and
performance assessment
impacts of DPC disposal in
various host rock environments***

Spent Fuel and Waste Disposition

***Prepared for
U.S. Department of Energy
Spent Fuel and Waste Science
and Technology
Jonny Rutqvist***

Lawrence Berkeley National Laboratory

June 26, 2020

LBNL-2001340

SFWD Working Document: External Release

CONTEXT FOR THIS STUDY

This is a technical paper that does not take into account contractual limitations or obligations under the Standard Contract for Disposal of Spent Nuclear Fuel and/or High-Level Radioactive Waste (Standard Contract) (10 CFR Part 961). For example, under the provisions of the Standard Contract, spent nuclear fuel in multi-assembly canisters is not an acceptable waste form, absent a mutually agreed to contract amendment.

To the extent discussions or recommendations in this paper conflict with the provisions of the Standard Contract, the Standard Contract governs the obligations of the parties, and this paper in no manner supersedes, overrides, or amends the Standard Contract.

This paper reflects technical work, which could support future decision making by DOE. No inferences should be drawn from this paper regarding future actions by DOE, which are limited both by the terms of the Standard Contract and a lack of Congressional appropriations for the Department to fulfill its obligations under the Nuclear Waste Policy Act including licensing and construction of a spent nuclear fuel repository.

DISCLAIMER

This document was prepared as an account of work sponsored by the United States Government. While this document is believed to contain correct information, neither the United States Government nor any agency thereof, nor the Regents of the University of California, nor any of their employees, makes any warranty, express or implied, or assumes any legal responsibility for the accuracy, completeness, or usefulness of any information, apparatus, product, or process disclosed, or represents that its use would not infringe privately owned rights. Reference herein to any specific commercial product, process, or service by its trade name, trademark, manufacturer, or otherwise, does not necessarily constitute or imply its endorsement, recommendation, or favoring by the United States Government or any agency thereof, or the Regents of the University of California. The views and opinions of authors expressed herein do not necessarily state or reflect those of the United States Government or any agency thereof or the Regents of the University of California.

This page is intentionally left blank.

Revision 6
10/07/2019**APPENDIX E****NTRD DOCUMENT COVER SHEET ¹**

Name/Title of Deliverable/Milestone/Revision No.	Geotechnical and performance assessment impacts of DPC disposal in various host rock environments/ M4SF-20LB010305042
Work Package Title and Number	Direct Disposal of Dual-Purpose Canisters - LBNL SF-20LB01030504
Work Package WBS Number	1.08.01.03.05
Responsible Work Package Manager	Jonny Rutqvist (signature on file) (Name/Signature)

Date Submitted **6/26/2019**

Quality Rigor Level for Deliverable/Milestone ²	<input type="checkbox"/> QRL-1 <input type="checkbox"/> Nuclear Data	<input type="checkbox"/> QRL-2	<input type="checkbox"/> QRL-3	<input checked="" type="checkbox"/> QRL 4 Lab-specific ³
--	---	--------------------------------	--------------------------------	--

This deliverable was prepared in accordance with Lawrence Berkeley National Laboratory (LBNL)
(Participant/National Laboratory Name)

QA program which meets the requirements of
 DOE Order 414.1 NQA-1 Other

This Deliverable was subjected to: Technical Review**Technical Review (TR)****Review Documentation Provided**

- Signed TR Report or,
 Signed TR Concurrence Sheet or,
 Signature of TR Reviewer(s) below

Name and Signature of Reviewers

Mengsu Hu

(Signature on file)

Boris Faybishenko: All Sections

(Signature on file)

 Peer Review**Peer Review (PR)****Review Documentation Provided**

- Signed PR Report or,
 Signed PR Concurrence Sheet or,
 Signature of PR Reviewer(s) below

Name and Signature of Reviewers

NOTE 1: Appendix E should be filled out and submitted with each deliverable. Or, if the PICS:NE system permits, completely enter all applicable information in the PICS:NE Deliverable Form. The requirement is to ensure that all applicable information is entered either in the PICS:NE system or by using the FCT Document Cover Sheet.

- In some cases there may be a milestone where an item is being fabricated, maintenance is being performed on a facility, or a document is being issued through a formal document control process where it specifically calls out a formal review of the document. In these cases, documentation (e.g., inspection report, maintenance request, work planning package documentation or the documented review of the issued document through the document control process) of the completion of the activity, along with the Document Cover Sheet, is sufficient to demonstrate achieving the milestone.

NOTE 2: If QRL 1, 2, or 3 is not assigned, then the QRL 4 box must be checked, and the work is understood to be performed using laboratory specific QA requirements. This includes any deliverable developed in conformance with the respective National Laboratory / Participant, DOE or NNSA-approved QA Program

NOTE 3: If the lab has an NQA-1 program and the work to be conducted requires an NQA-1 program, then the QRL-1 box must be checked in the work Package and on the Appendix E cover sheet and the work must be performed in accordance with the Lab's NQA-1 program. The QRL-4 box should not be checked

This page is intentionally left blank.

TABLE OF CONTENTS

TABLE OF CONTENTS.....	v
LIST OF FIGURES	vi
LIST OF TABLES.....	viii
ACRONYMS.....	ix
1. INTRODUCTION.....	1
2. MODEL SETUP.....	5
3. FUNCTION OF THERMALLY ENGINEERED BACKFILL	11
4. DUCTILE VERSUS BRITTLE SHALE THM RESPONSE.....	13
4.1 Nominal Emplacement Drifts Spacing of 40 m	13
4.2 Drift Spacing Extended to 100 m.....	16
5. EBS DESIGN WITH CONCENTRIC CANISTER LOCATION	19
5.1 24-PWR DPCs 100YOoR and High Thermal Conduction Bentonite Properties	20
5.2 37-PWR DPCs 100YOoR and Increased Drift Spacing	21
6. SUMMARY OF FY20 PROGRESS AND FUTURE WORK.....	25
7. ACKNOWLEDGEMENTS	27
8. REFERENCES	29

LIST OF FIGURES

Figure 1-1. Schematic of repository-scale coupled thermo-hydro-mechanical responses and their impacts on emplacement tunnels (Rutqvist, 2020).....	2
Figure 2-1. Three-dimensional model geometry of a horizontal emplacement tunnel in the middle of a repository with a 20 m center-to-center spacing between individual DPCs and a 40 m spacing between individual emplacement tunnels. (a) Tunnel side and front views illustrating the symmetric temperature evolution with a numerical grid and a 3D view shown in (b) and (c).....	8
Figure 2-2. Modeling steps: from tunnel excavation to post-closure period.	9
Figure 2-3. Decay heat functions for various DPC packages and surface decay storage times displayed (a) over time (linear scale) to 1000 years, and (b) over time (logarithmic scale) to 100,000 years (Rutqvist, 2020). The data are derived from Carter et al., (2013).....	10
Figure 3-1. Calculated (a) temperature and (b) liquid saturation 10 years after emplacement for thermally engineered (left) and conventional bentonites (right) for a repository tunnel in argillite and decay heat from a 24-PWR-DPC emplaced at 100yOoR (Rutqvist, 2020).....	11
Figure 4-1. Results of temperature evolution for (a) ductile and (b) brittle shale.....	14
Figure 4-2. Results of simulations of the pressure evolution for (a) ductile and (b) brittle shales.	14
Figure 4-3. Results of simulations of the evolution of horizontal compressive stress and strength for shear along existing fractures for (a) ductile and (b) brittle shales.	15
Figure 4-4. Results of simulations of the evolution of the tangential and radial stress evolutions on top of emplacement tunnel and the potential for compressive or tensile failure for (a) ductile and (b) brittle shales.....	15
Figure 4-5. Results of simulations of the temperature evolution for (a) ductile and (b) brittle shale for a drift spacing extended to 100 m.	16
Figure 4-6. Results of simulations of the pressure evolution for (a) ductile and (b) brittle shales for a drift spacing extended to 100 m.	17
Figure 4-7. Results of simulations of the evolution of a horizontal compressive stress and strength for shear along existing fractures for (a) ductile and (b) brittle shales, for a drift spacing extended to 100 m.....	17
Figure 4-8. Results of simulations of tangential and radial stress evolutions on the top of the emplacement tunnel and the potential for compressive or tensile failure for (a) ductile and (b) brittle shales for a drift spacing extended to 100 m.....	18
Figure 5-1. The Swiss concept of an emplacement tunnel with bentonite backfill and the canister placed on a pedestal of bentonite blocks (a), and an upscale version (b) that could potentially be applied for large scale canisters.	19
Figure 5-2. Results of simulations of the temperature evolution for (a) ductile and (b) brittle shales for concentric canister emplacement and a 100 m drift spacing.	20
Figure 5-3. Results of simulations of the saturation evolution for (a) ductile and (b) brittle shales for concentric canister emplacement and a 100 m drift spacing.....	21

Figure 5-4. Results of simulations of the pressure evolution for (a) ductile and (b) brittle shales for concentric canister emplacement and a 100 m drift spacing..... 21

Figure 5-5. Results of simulations of the pressure evolution for (a) ductile and (b) brittle shales for concentric canister emplacement and a 100 m drift spacing..... 23

Figure 5-6. Results of simulations of the pressure evolution for (a) ductile and (b) brittle shales for concentric canister emplacement and a 100 m drift spacing..... 23

LIST OF TABLES

Table 2-1. Basic THM properties of host rocks and a concrete liner.....	7
Table 2-2. THM properties for the bentonite buffer representing FEBEX bentonite with simplification such a linear swelling and linear saturation dependent thermal conductivity (Rutqvist et al., 2011)	9
Table 2-3. Decay heat sources for various DPC packages and surface decay storage times. The data for the decay heat are derived from Carter et al., (2013).	10

ACRONYMS

DECOVALEX	DEvelopment of COupled Models and their VALidation against Experiments
DOE	Department of Energy
DPC	Dual-Purpose Canister
EBS	Engineered barrier system
FEBEX	Full-scale Engineered Barrier Experiment
FLAC	Fast Lagrangian analysis of continua
FY	Fiscal year
GDSA	Geologic Disposal Systems Analysis
LBNL	Lawrence Berkeley National Laboratory
PWR	Pressurized Water Reactor
SNF	Spent Nuclear Fuel
SFWD	Spent Fuel and Waste Disposition
THM	Thermo-hydro-mechanical
TOUGH	Transport of Unsaturated Groundwater and Heat
UFD	Used Fuel Disposition
yOoR	years-Out-of-Reactor

This page is intentionally left blank.

GEOMECHANICAL AND PERFORMANCE ASSESSMENT IMPACTS OF DPC DISPOSAL IN VARIOUS HOST ROCK ENVIRONMENTS

1. INTRODUCTION

The report presents the progress of research activity addressing geotechnical and performance assessment impacts of direct disposal of commercial spent nuclear fuel (SNF) in dual-purpose canisters (DPCs) in various host rock environments. Previous studies on direct disposal of DPC within the Department of Energy's (DOE) Spent Fuel and Waste Disposition (SFWD) campaign found that direct disposal is technically feasible for most DPCs, depending on the repository host geology (Hardin et al., 2015). Post closure criticality controls and thermal management strategies, which allow for permanent disposal within 150 years (after taken out of the reactor), were identified as two of the most challenging aspects (Hardin et al., 2015). The DPCs are currently also being considered in the geologic disposal system analysis (GDSA) within the SFWD campaign. In GDSA, heat sources from either 24-PWR or 37-PWR DPCs are considered with a decay storage time varying from 50 to 150 years before disposal. The GDSA modeling is being conducted using large-scale models focusing on the radionuclide transport to accessible environments, and includes repository-scale coupled thermal-hydraulic processes. Previous studies on DPC thermal managements and the current GDSA work provide the basic background for the study on the geomechanical impact of direct DPC disposal.

DPCs containing 24 Pressurized Water Reactor (PWR) fuel elements are common, and DPCs may contain up to 37 PWR elements in the future (Hardin et al., 2013). DPCs with up to 37 PWR elements are very large compared to conventional disposal canisters, compared to those used in the Swedish KBS-3 concept, containing just 4 PWR elements (Posiva SKB, 2017). Since the amount of heat released due to decay of radioactive waste from a specific waste canister depends on the number of spent fuel elements, very high temperature could be expected around DPCs containing either 24 or 37 PWR elements. As a result, post-closure thermal management strategies that allow for disposal within 150 years (after taken out from the reactor) have been identified as one of the challenging aspects of direct DPC disposal (Hardin et al., 2015). Thermal management strategies include keeping emplacement tunnels open with ventilation for decades, because a backfill generally leads to a substantial increase in temperature at the waste package. Thus, it is not clear whether a multi-barrier repository design with bentonite-backfilled tunnels is feasible for disposal of large size nuclear waste canisters.

The FY19 milestone report (Rutqvist, 2019) focused on scoping calculations to identify some of the most important geomechanical impacts of direct disposal of SNF in DPCs. Previously developed and tested modeling approaches, based on the TOUGH-FLAC simulator, were applied with detailed representation of the near-field coupled processes (Rutqvist et al., 2011; 2014; 2019; 2018). Moreover, the use of a thermally engineered backfill for reducing and controlling the relatively short-term (tens of years) buffer peak temperature was investigated. The results from published laboratory experiments have shown that the thermal conductivity of bentonite can be significantly increased by mixing in graphite or graphene oxide (Chen et al., 2018). Moreover, the results were generalized by studying two different host rock types: softer argillaceous clay (or argillite) and hard crystalline (granite) host rocks. The work presented in Rutqvist (2019) was developed into a journal publication with the external technical peer-review, and an article has been recently published in "Tunneling and Underground Space Technology" (Rutqvist, 2020). The paper

highlights the results that the use of a backfill that is thermally engineered for high heat conduction can reduce the EBS temperature to acceptable levels to allow for disposal of large waste canisters in backfilled tunnels. On the other hand, the use of high heat conduction backfill will not reduce the far field rock peak temperature that can occur several thousand years after closure of the repository. This longer-term host rock peak temperature generates thermal-poro-elastic stress and geomechanical changes that must be considered in the thermal management and design of a repository.

The researches presented in Rutqvist (2019; 2020) confirm the importance of the repository temperature in creating a thermal stress and thermal pressurization, which if not managed, could lead to wide-spread fracturing or shear activation of fractures and faults, as well as a high stress concentration and damage around emplacement tunnels (Figure 1-1). Because the vertical stress remains constant and equal to the weight of the overburden, thermally-induced horizontal stress will result in an increased shear stress that will be the driver for potential activation of fractures and faults (Figure 1-1a). Such shear activation could result in an increased permeability and could also potentially induce small seismic events. Finally, the increasing horizontal stress will act on the repository tunnels, and stress concentration around the tunnel openings could cause a compressive spalling failure or tensile failure of different parts of the tunnel walls (Figure 1-1b). These are thermally-induced coupled THM processes that need to be evaluated in the thermal management of a nuclear waste repository over a post-closure period of up to 100,000 years.

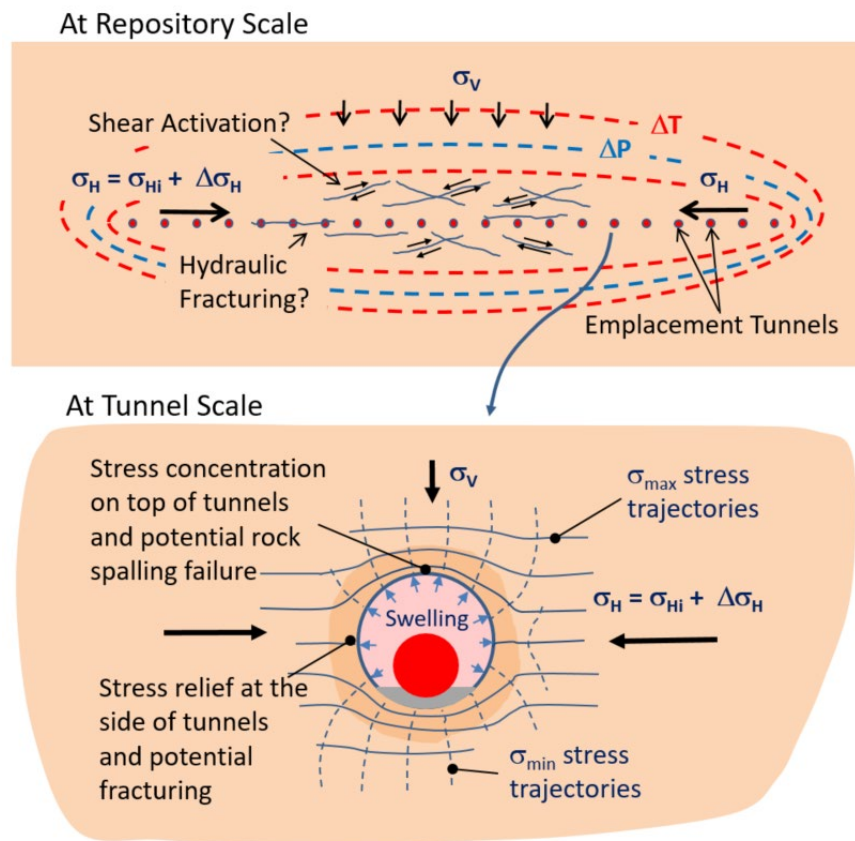


Figure 1-1. Schematic of repository-scale coupled thermo-hydro-mechanical responses and their impacts on emplacement tunnels (Rutqvist, 2020).

This report presents updated results of the geomechanical and performance assessment impacts of DPC disposal in various host rock environments, different EBS designs and different host rock properties. In the FY19, two different host properties representing argillite (Opalinus Clay) and granite was considered. Here, two endmembers of argillite are considered, representing more ductile shale similar to that of Pierre Shale, and more brittle shale similar to that of Palezoic shales in the eastern U.S (Perry et al., 2014; Dobson and Houseworth, 2014). The more brittle shales generally have significantly different properties than the more ductile shales, such as Opalinus Clay. They are stronger and stiffer, with higher thermal conductivity and may be fractured causing higher permeability (Perry et al., 2014; Dobson and Houseworth, 2014). Regarding repository design, an alternative design is considered where the nuclear waste package emplaced concentrically at the center of the emplacement tunnel.

This page is intentionally left blank.

2. MODEL SETUP

Figures 2-1 and 2-2 present the basic model geometry used for simulating disposal at a 500 m depth. The model was developed and applied in FY19 and described in the FY19 milestone report (Rutqvist, 2019) and in a recently published journal article (Rutqvist, 2020). A three-dimensional symmetric model is constructed around a single DPC to represent the evolution for an emplacement tunnel at the inner part of a repository, where the highest temperature changes and a thermal impact could be expected (Figure 2-1). The initial 3D model is built for a canister-to-canister spacing of 20 m along the emplacement tunnels and a 40 m spacing between individual emplacement tunnels (Figure 2-1a). The DPCs with overpack (5.6 m long and 2 m in diameter) are placed on the floor of the emplacement tunnels of about 4.5 m in diameter (Hardin et al., 2013; 2014). The DPCs are assumed to have THM properties corresponding to steel, including Young's modulus $E = 210$ GPa, Poisson's ratio $\nu = 0.3$, thermal conductivity of $\lambda = 0.3$, and specific heat $C_s = 500$ J/kg \cdot °C. As an option, the tunnels may be assumed to be reinforced with a concrete liner and the DPCs are placed on a concrete invert on the tunnel floor.

As a result of the repetitive symmetry, boundary conditions on the lateral boundaries of the 3D model are no heat or fluid flow and no displacements normal to the boundaries. On the top and bottom boundaries, temperature and fluid pressure are fixed, with vertical displacement fixed to zero on the bottom and free to move on the upper boundary representing the free moving ground surface. Further, the repetitive symmetry assumes that all neighboring DPCs are emplaced simultaneously to account for heat impacting neighboring DPCs.

Some of the basic THM properties for the host rocks and a concrete liner are listed in Table 1-1. In the FY19 report, properties for Opalinus Clay were used to represent repository in argillite, while an alternative scenario of a repository in crystalline rock was also considered. Here in the FY20 report, two endmembers of argillite properties are considered, representing ductile shale, such as Pierre Shale, and a more brittle shale, such as Marcellus shale in the eastern U.S. (Perry et al., 2014; Dobson and Houseworth, 2014). In the current study, one set of typical properties is selected for ductile and brittle shale, whereas in reality the properties of each type of shale vary widely (Dobson and Houseworth, 2014).

The backfill for the buffer is assumed to consist of the bentonite used in the Full-scale Engineered Barriers Experiment (FEBEX) at the Grimsel Test Site in Switzerland (Alonso et al., 2005; Gens et al., 2009). The bentonite THM model used here is the same as that used and presented in Rutqvist et al. (2011) with parameters listed in Table 1-2. In this study, the simpler linear swelling for the bentonite buffer was considered to provide a 5 MPa swelling stress at full saturation (Rutqvist et al., 2011). The linear swelling model adds a swelling strain, $\Delta\varepsilon_{sw}$, according to $\Delta\varepsilon_{sw} = \Delta S_l \times \beta_{sw}$, where ΔS_l is change in liquid saturation, and β_{sw} is a moisture swelling coefficient. The bulk modulus of 20 MPa and β_{sw} of about 5 MPa are used for calculations when the full saturation is achieved. The parameters for the water retention curve and relative permeability, which are listed in Table 2-2, were determined through back-analysis modeling of laboratory experiments conducted on the FEBEX bentonite (Alonso et al., 2005).

A thermally engineered backfill is considered here based on the results in FY19 milestone report (Rutqvist, 2019). Based on the FEBEX bentonite properties, in the numerical model, the thermal conductivity is linearly dependent on saturation varying from $\lambda_{dry} = 0.5$ W/mK (at zero liquid saturation) to $\lambda_{wet} = 1.3$ W/mK (at full liquid saturation). Simulations were conducted considering thermally engineered backfill material, i.e., a high heat conduction buffer material with $\lambda_{dry} = 5$ W/mK and $\lambda_{wet} = 10$ W/mK. These values are based on the recently published laboratory results by Chen et al., (2018), showing that thermal conductivity of bentonite could be increased by as much as an order of magnitude using admixtures of graphene oxide. In other simulations, the graphite admixture was represented by $\lambda_{dry} = 1$ W/mK and $\lambda_{wet} = 3.2$ W/mK (Rutqvist, 2019).

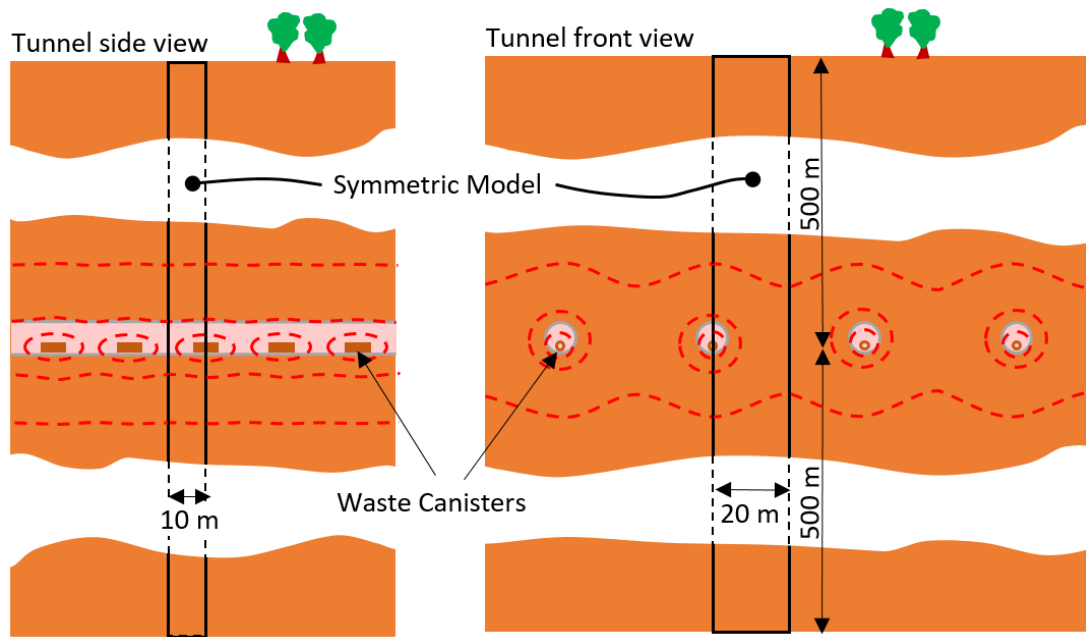
For initial conditions, hydrostatic fluid pressure and a thermal gradient of 28°C per km were assigned. With the ground water table near the ground surface and a ground surface temperature of 10°C, the initial pressure and temperature at 500 m depth was about 4.5 MPa and 24°C, respectively. Isotropic stress field was assumed with the magnitude of the three principal stresses being equal to the weight of the overburden rock.

The modeling steps included excavation, reinforcement, emplacement of the waste canisters and buffer, followed by the post-closure simulation over 100,000 years (Figure 2-2). It is assumed that the waste canister and buffer are installed at an instant defined as time zero in the post-closure simulations. The buffer is installed at an initial liquid saturation of 65%. Sevougian et al. (2019) developed several options of decay heat functions representative of existing and future inventories of DPCs on the basis of radionuclide inventories in Carter et al. (2013), including both 24-PWR and 37-PWR DPCs with a decay storage of up to 150 years before disposal (Table 2-1). In the model simulations performed in the current study, the two endmembers of 24-PWR DPC were emplaced after 100 years-Out-of-the-Reactor (yOoR) and 37-PWR DPC were emplaced at 100 years. The decay functions for the 37-PWR DPCs are developed from Carter et al. (2013) considering fuel elements with relatively high burn-up of 60 GWd/MTU (gigawatt-days/metric ton of uranium), which resulted in a relatively high initial decay heat. In Table 2-1, note the big difference in initial decay heat for 100 versus 150 yOoR, but in 1000 years the decay heat is expected almost the same, but would still remain above 1000 W. This is clearly shown in Figure 2-3, which presents the heat decay function over time for the first 1000 years (Figure 2-3a) for 100,000 years (Figure 2-3b).

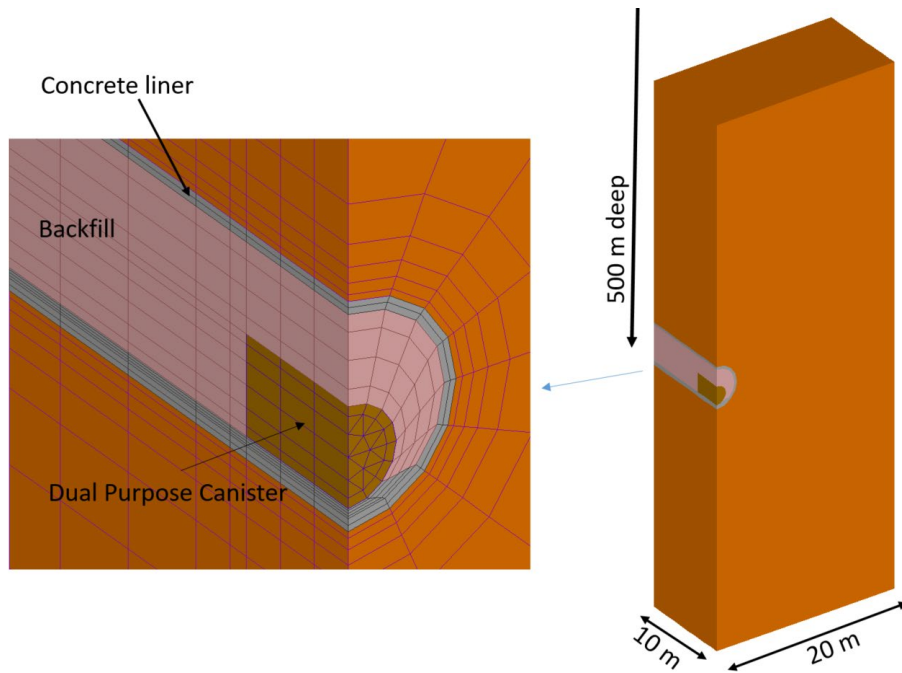
In the post-closure simulations, the geomechanical impacts are evaluated in terms of the stress evolution at the repository level away from the emplacement tunnels, as well as at the tunnel walls, where the stress concentrations are the highest. The stress-strain evolution is calculated considering linear poro-elasticity and thermo-elasticity, whereas the potential for failure is considered through stress criteria. For the repository level stresses, simple criteria are the tensile stress could induce tensile failure, while a shear stress equals to or larger than the shear strength could induce shearing of pre-existing fractures (Rutqvist et al., 2014). For the top and bottom of the emplacement tunnels, where the highest compressive tangential stress is expected to occur, a spalling failure criterion is considered through a uniaxial compressive strength.

Table 2-1. Basic THM properties of host rocks and a concrete liner

Parameter	Argillite (Opalinus)	Ductile Shale (Pierre)	Crystalline (Granite)	Brittle Shale (Marcellus)	Concrete
Bulk Density [kg/m ³]	2400	2300	2700	2600	2700
Porosity [-]	0.15	0.2	0.01	0.10	0.15
Young's Modulus [GPa]	5	3	35	30	23
Poisson's ratio [-]	0.3	0.3	0.3	0.2	0.2
Grain Specific heat [J/kg·°C]	900	900	900	900	900
Thermal conductivity [W/m·°C]	1.7	1.2	3.0	1.7	2.0
Thermal expansion coefficient [°C ⁻¹]	1.0×10 ⁻⁵	1.0×10 ⁻⁵	1.0×10 ⁻⁵	1.0×10 ⁻⁵	1.0×10 ⁻⁶
Bulk Permeability [m ²]	5.0×10 ⁻²⁰	1.0×10 ⁻²⁰	1.0×10 ⁻¹⁷	1.0×10 ⁻¹⁹	1.0×10 ⁻¹⁹



(a)



(b)

(c)

Figure 2-1. Three-dimensional model geometry of a horizontal emplacement tunnel in the middle of a repository with a 20 m center-to-center spacing between individual DPCs and a 40 m spacing between individual emplacement tunnels. (a) Tunnel side and front views illustrating the symmetric temperature evolution with a numerical grid and a 3D view shown in (b) and (c).

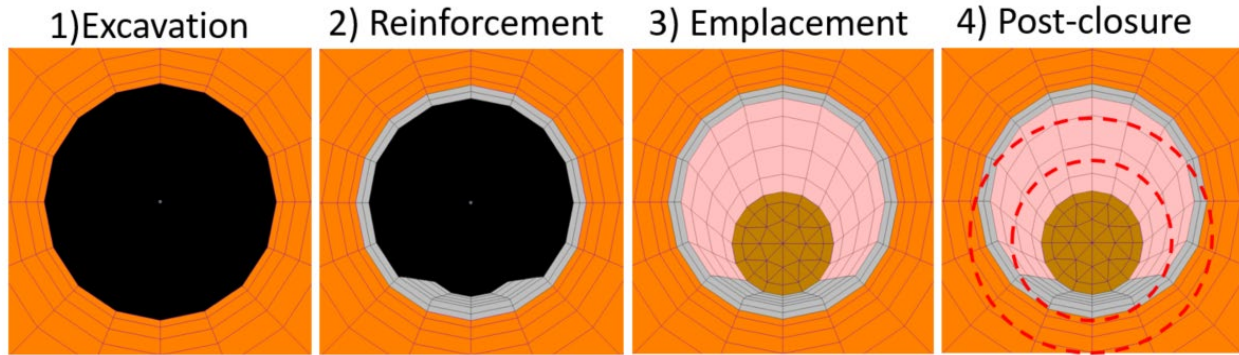


Figure 2-2. Modeling steps: from tunnel excavation to post-closure period.

Table 2-2. THM properties for the bentonite buffer representing FEBEX bentonite with simplification such a linear swelling and linear saturation dependent thermal conductivity (Rutqvist et al., 2011)

Parameter	Value/Function
Initial dry density, ρ_d [kg/m ³]	$1.6 \cdot 10^3$
Initial porosity, ϕ [-]	0.41
Saturated permeability, k [m ²]	$2.0 \cdot 10^{-21}$
Relative permeability, k_r [-]	$k_{rl} = S_l^3$
Van Genuchten's (1980) parameter, P_{VG} [MPa]	30
Van Genuchten's (1980) parameter, λ_{VG} [-]	0.32
Thermal expansion, β [1/°C]	$1.5 \cdot 10^{-4}$
Grain specific heat, C_s [J/kg·°C]	800
Thermal conductivity, λ_m [W/m·°C]	$\lambda_m = \lambda_{dry} + S_l \times (\lambda_{wet} - \lambda_{dry})$
Molecular diffusion coefficient, D_{v0} [m ² /s]	$2.16 \cdot 10^{-5}$
Mass flow times tortuosity factor, τ [-]	0.8
Bulk modulus, K [MPa]	20
Poisson's ratio, [-]	0.35
Moisture swelling coefficient, β_{sw}	0.238

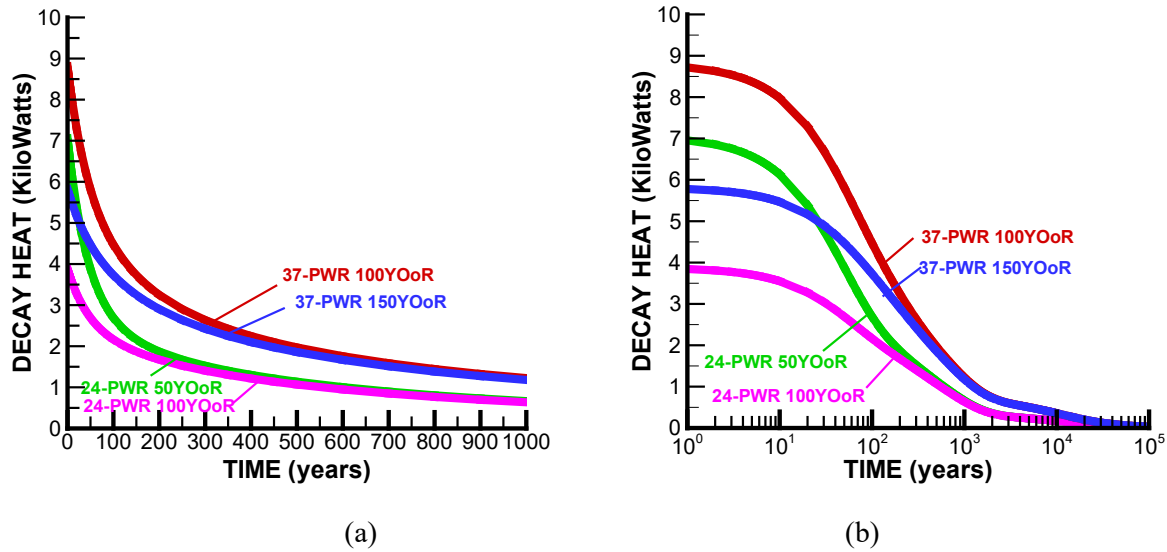


Figure 2-3. Decay heat functions for various DPC packages and surface decay storage times displayed (a) over time (linear scale) to 1000 years, and (b) over time (logarithmic scale) to 100,000 years (Rutqvist, 2020). The data are derived from Carter et al., (2013).

Table 2-3. Decay heat sources for various DPC packages and surface decay storage times. The data for the decay heat are derived from Carter et al., (2013).

DPC heat source name for the model	Burn-Up (GWd/MT)	Enrichment (%)	Number of PWR fuel elements per DPC	Surface Decay Storage Time (Years)	Decay Heat (Watts)	
					At disposal	1000 Years
24-PWR 50YOoR	40	3.72	24	50	7057	66
24-PWR 100YOoR	40	3.72	24	100	3881	64
37-PWR 100YOoR	60	4.73	37	100	8810	1224
37-PWR 150YOoR	60	4.73	37	150	5817	1179

3. FUNCTION OF THERMALLY ENGINEERED BACKFILL

The FY19 modeling study published in Rutqvist (2020) provided new insight into thermal management associated geologic disposal of large disposal canisters, such as DPCs. Importantly, the study demonstrated the feasibility of disposal of very large nuclear waste canisters in bentonite-backfilled tunnels. This can be accomplished by the use of bentonite engineered with high heat conduction, such that the high amount of decay heat from large disposal canisters can be efficiently transferred into the surrounding host rock. The way this works is illustrated in Figure 3-1 from Rutqvist (2020), comparing the distributions of temperature and saturation at 10 years after emplacement of the canister.

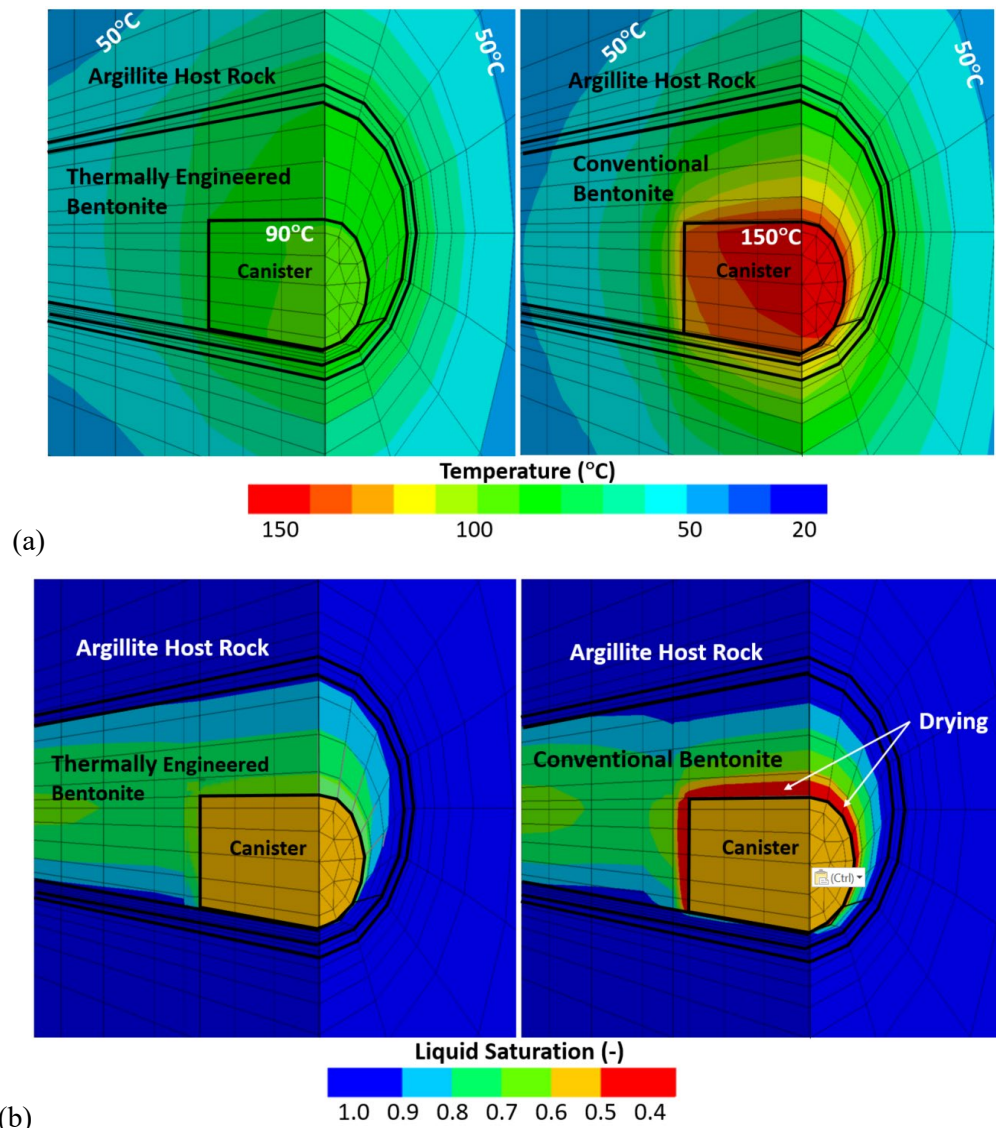


Figure 3-1. Calculated (a) temperature and (b) liquid saturation 10 years after emplacement for thermally engineered (left) and conventional bentonites (right) for a repository tunnel in argillite and decay heat from a 24-PWR-DPC emplaced at 100yOoR (Rutqvist, 2020).

With a buffer thermally engineered for high heat conduction, the heat can be effectively transferred to other parts of the bentonite buffer and then released into the surround host rock (Figure 3-1a). The largely reduced thermal gradient across the buffer do also eliminate evaporation drying (and any potential desiccation fractures) near the waste canister, which can actually accelerate resaturation and swelling of the buffer (Figure 3-1b). It is important to develop a swelling stress to assure the protective function of the buffer and eliminate any voids that otherwise could host microbial activities.

4. DUCTILE VERSUS BRITTLE SHALE THM RESPONSE

In this section, the THM responses for more ductile or brittle shales are compared. The same repository design is considered for the two cases, with the only difference being the host rock properties. Here, the conventional FEBEX bentonite properties are used with the original thermal conductivity.

4.1 Nominal Emplacement Drifts Spacing of 40 m

Figures 4-1 and 4-2 show the temperature and pressure evolutions for the two cases. In the case of ductile shale, the peak temperatures are higher and associated thermal pressurization is much higher. The peak temperature is higher in a case of the ductile shale, because the thermal conductivity is lower. The temperature is well over 100°C at the inner part of the bentonite for up to 1000 years. Note that in this case, simulations were conducted using conventional values of thermal conductivity of the bentonite. As discussed above, the peak temperature at the inner parts of the buffer could be effectively reduced by using a thermally engineered bentonite material.

Figure 4-2 shows that the thermal pressurization and peak pressure is much higher in the case of the ductile shale. It is higher because of a higher and steeper temperature rise in combination with lower permeability. In both cases, simulations show that fluid pressure could increase to levels above the lithostatic stress and could therefore potentially induce hydraulic fracturing. Such high thermal pressurization may be avoided by increasing the distance between individual emplacement tunnels, which will be shown in the next section.

Figure 4-3 shows the potential for shear activation of fractures in the repository host rock. As illustrated in Figure 1-1, shear activation could be induced on existing fractures that are favorably oriented for a shear slip. That would be shallow dipping fractures, dipping approximately 30 degrees from the horizontal. Figure 4-3 shows the potential for activation of such fractures or faults based on a Mohr-Coulomb criterion, and assuming that fractures of any orientation could exist at each point of space. If considering fractures or faults with zero cohesion and coefficient of friction of 0.6, the criterion is that a shear slip could potentially occur if the maximum compressive effective stress is 3 times larger than the minimum compressive effective stress (Rutqvist et al., 2014).

In Figure 4-3a we see that in the case of ductile shale, the effective compressive horizontal stress does not change very much, ranging from 5 to 10 MPa, whereas the compressive strength is decreasing below the effective compressive stress from about 100 to 10,000 years. The shear strength decreases because of thermal pressurization that tends to reduce the minimum compressive principal stress, which is the vertical effective stress. Note that this is the potential for shear activation, if fractures exist of such orientation. For a shale, fractures maybe be oriented parallel and normal to the bedding, and those fractures would not be favorably oriented for shear activation.

In the case of a brittle shale, as shown in Figure 4-3b, the horizontal compressive effective stress increases from 8 MPa to peak at 30 MPa at about 1000 years. This peak is caused by a thermal stress that is correlated with the temperature peak in the host rock. At the same time there is a reduction in the shear strength resulting from a reduction in the vertical effective stress along with the thermal pressurization. In this case there is a potential for fracture shear activation within a few tens of years after emplacement and this condition lasts for up to 10,000 years. The high shear stress prolonged for such a long time in a fractured rock mass could potentially induce shear activation and, perhaps, induce seismicity.

At the tunnel wall, on top of the emplacement tunnel, the stress evolution and potential for damage is quite different for cases of ductile and brittle shales. The ductile shale has very low uniaxial compressive strength

and therefore a compressive failure may already be induced due to excavation. For a brittle shale, the strength is much higher, but then the thermal stress and its concentration around the tunnel wall are also much higher. In the case of brittle shale for the condition considered here, damage may be induced on the top of the tunnel thousands of years after the closure of the repository. Again, such damage may be avoided by increasing the distance between individual emplacement tunnels, which will be demonstrated in the next section.

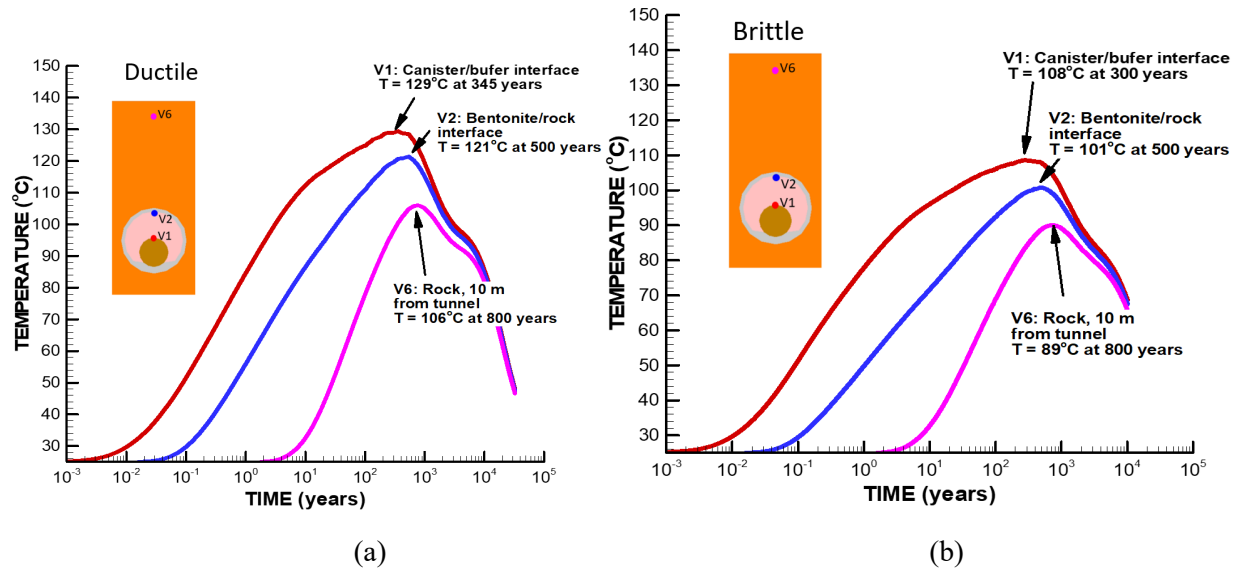


Figure 4-1. Results of temperature evolution for (a) ductile and (b) brittle shale.

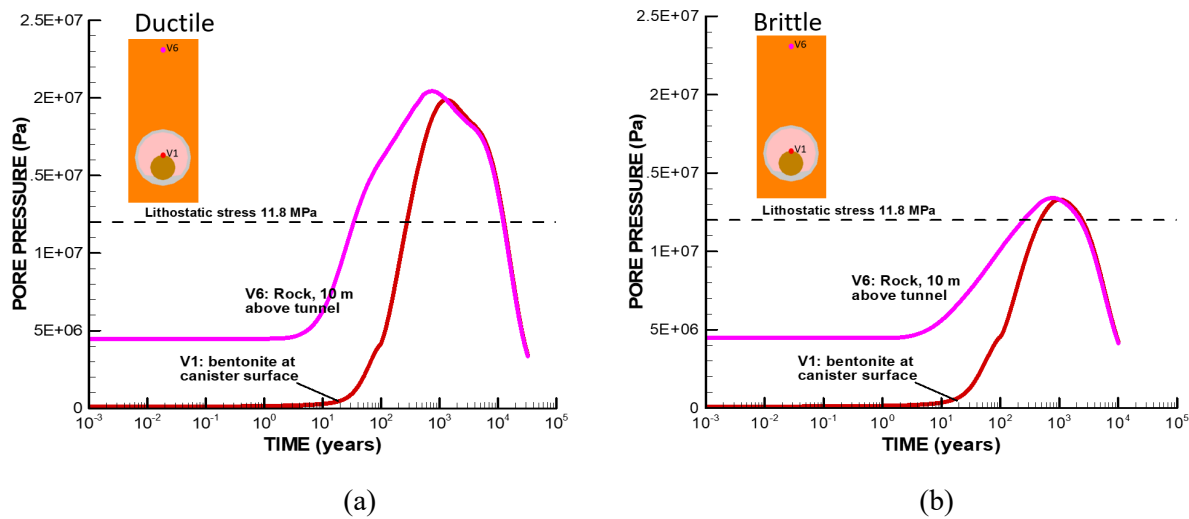


Figure 4-2. Results of simulations of the pressure evolution for (a) ductile and (b) brittle shales.

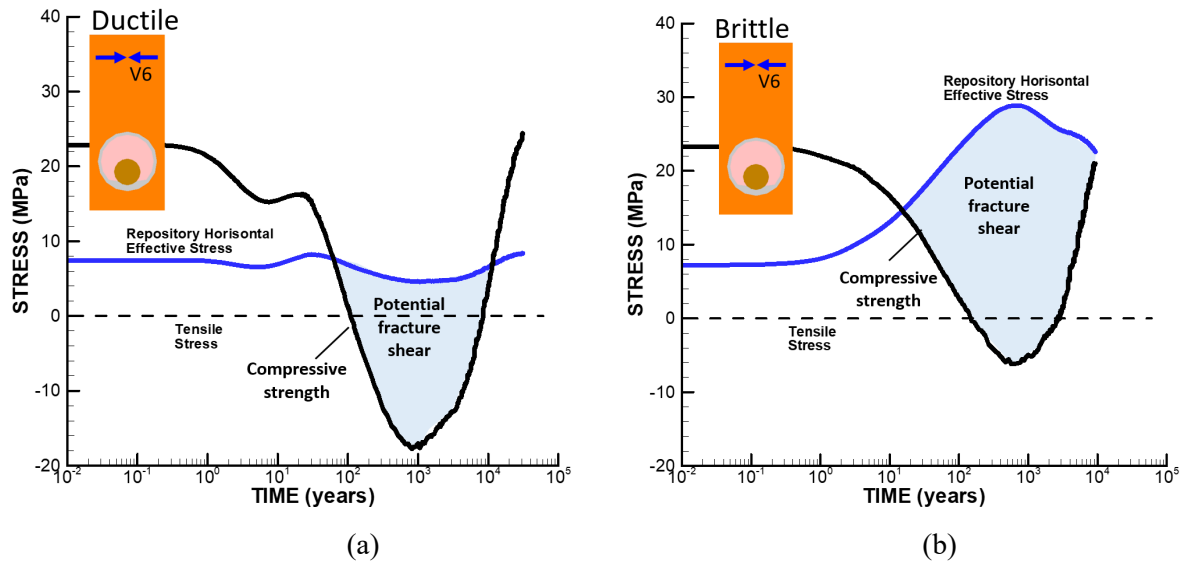


Figure 4-3. Results of simulations of the evolution of horizontal compressive stress and strength for shear along existing fractures for (a) ductile and (b) brittle shales.

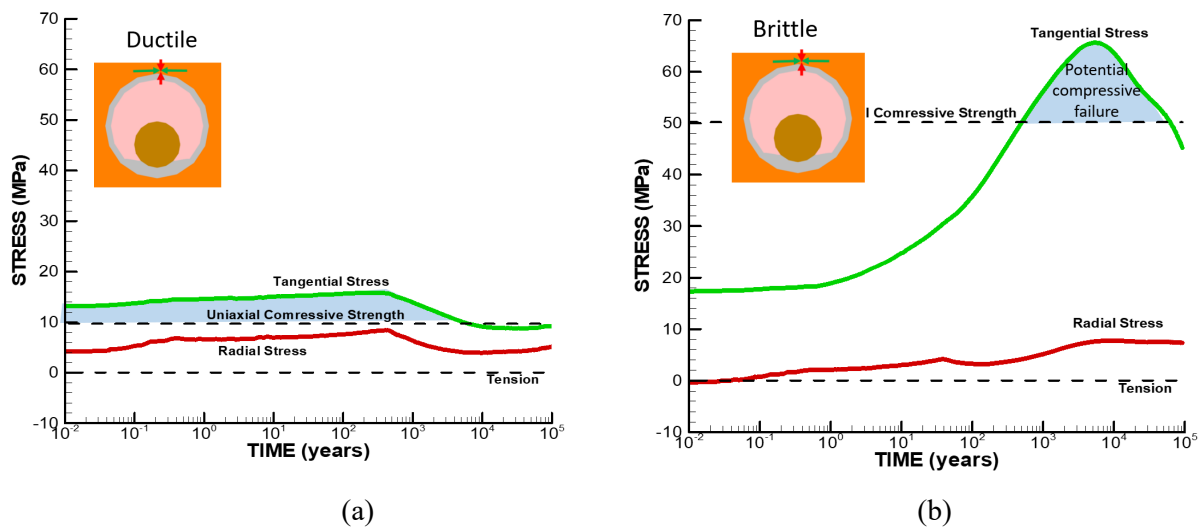


Figure 4-4. Results of simulations of the evolution of the tangential and radial stress evolutions on top of emplacement tunnel and the potential for compressive or tensile failure for (a) ductile and (b) brittle shales.

4.2 Drift Spacing Extended to 100 m

In this case, we considered a case of the extended spacing between emplacement tunnels, which increased from 40 m to 100 m. The results illustrated in Figures 4-5 through 4-8 show a reduced temperature, a much-reduced magnitude of thermal pressurization and a much-decreased potential for shear activation. The temperature at inner parts of the buffer peaked already after 20 years and then declined (Figure 4-5). The peak temperature was still well above 100°C, but this could be reduced further by applying materials with thermally engineered buffer properties.

Numerical simulations show that the thermal pressurization results in a peak fluid pressure that does not exceed the lithostatic stress, indicating no hydraulic fracturing (Figure 4-6). Also, the potential for shear activation is avoided in the case of a ductile host rock, and it substantially reduced in the case of a brittle host rock (Figure 4-7). Finally, the damage to the top of the excavation, that would occur thousands of years after the closure, can be avoided by increasing the drift spacing from 40 to 100 m (Figure 4-8). This model simulations show that the distance between individual emplacement tunnels represent a design parameter for evaluating how to avoid hydraulic fracturing or shear activation on existing fractures and to avoid thermal-mechanical damage to the excavation walls.

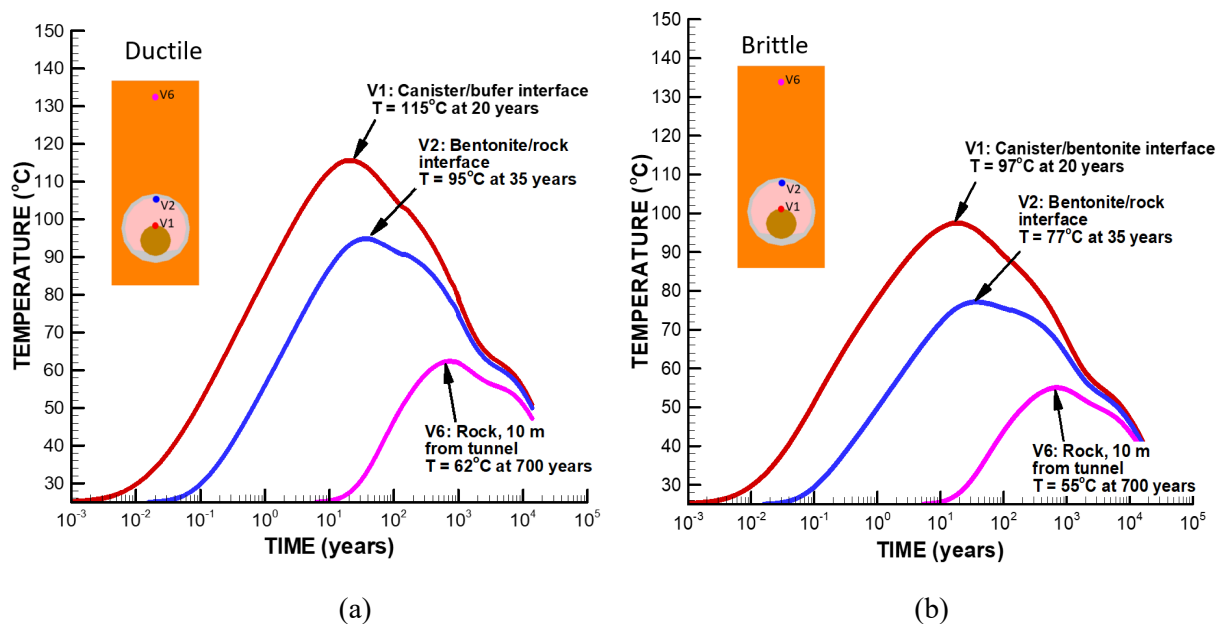


Figure 4-5. Results of simulations of the temperature evolution for (a) ductile and (b) brittle shale for a drift spacing extended to 100 m.

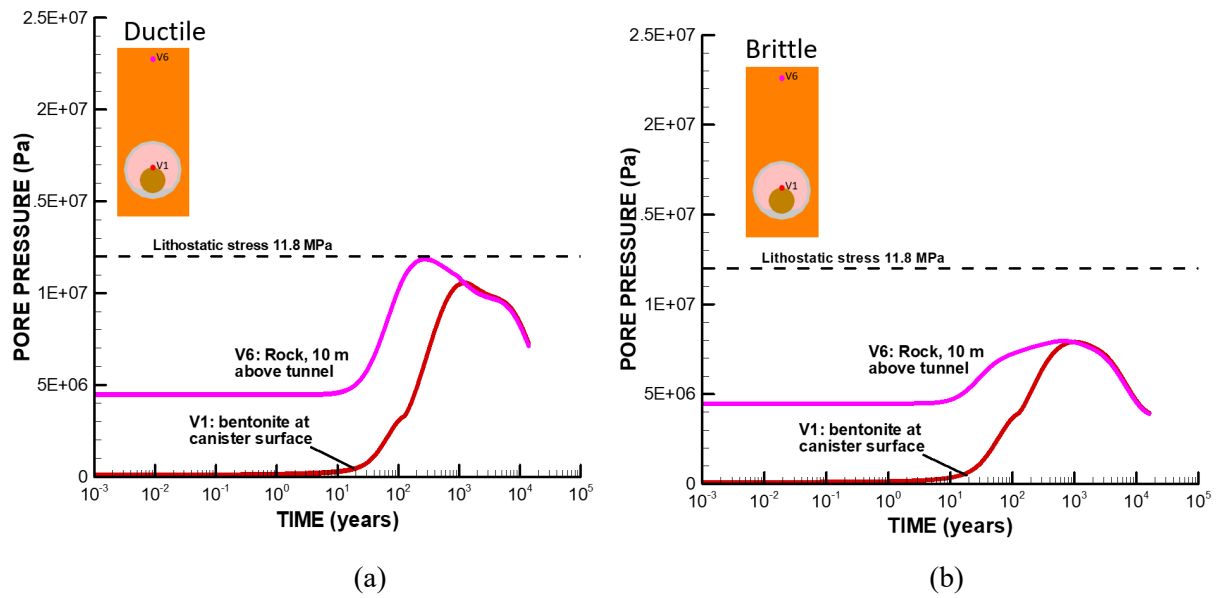


Figure 4-6. Results of simulations of the pressure evolution for (a) ductile and (b) brittle shales for a drift spacing extended to 100 m.

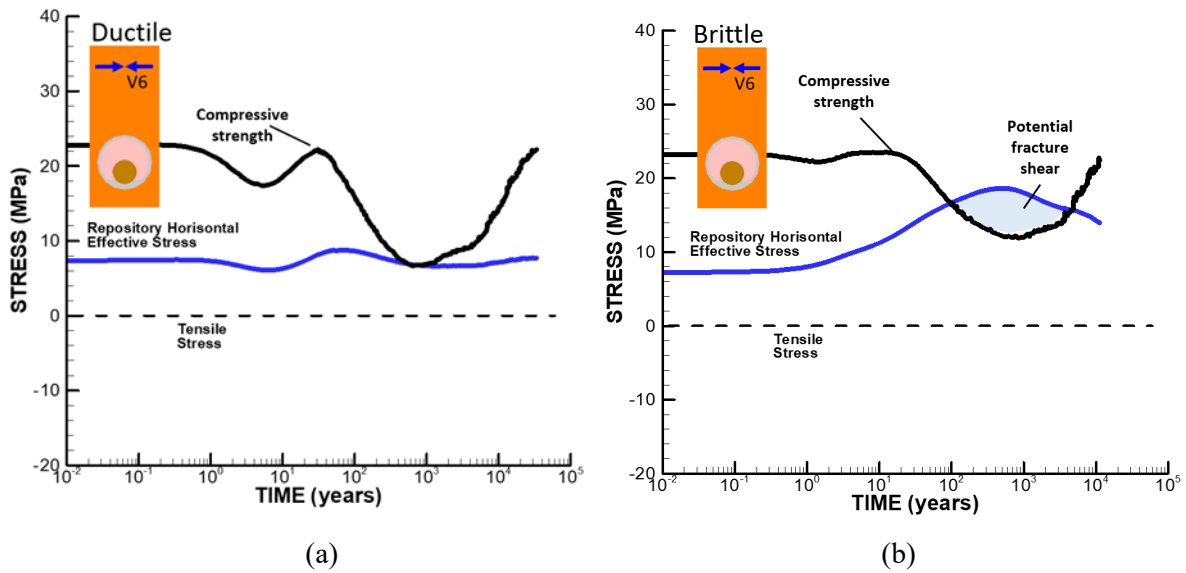


Figure 4-7. Results of simulations of the evolution of a horizontal compressive stress and strength for shear along existing fractures for (a) ductile and (b) brittle shales, for a drift spacing extended to 100 m.

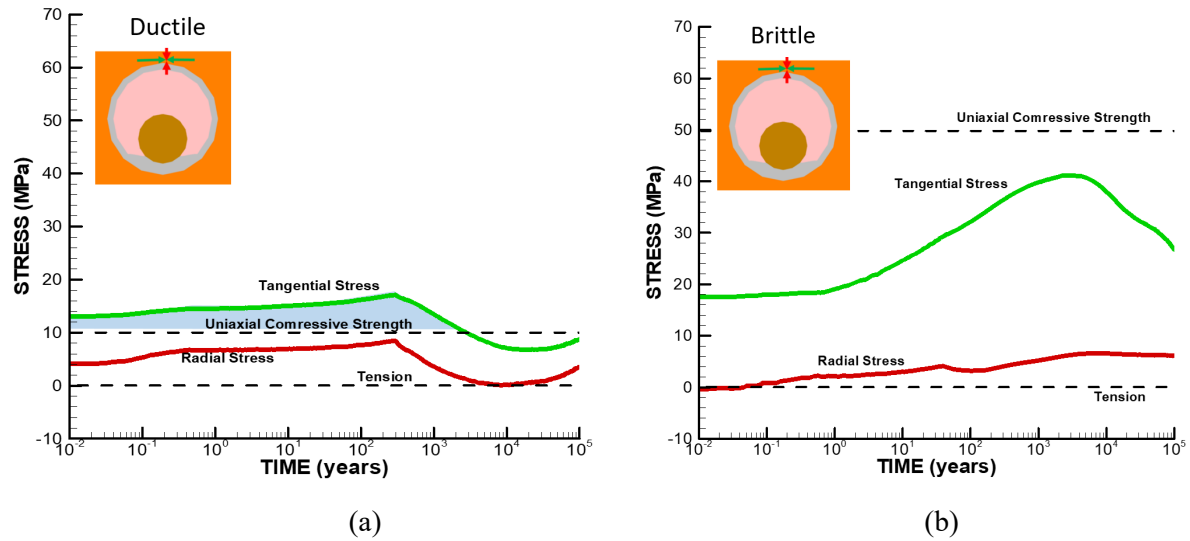


Figure 4-8. Results of simulations of tangential and radial stress evolutions on the top of the emplacement tunnel and the potential for compressive or tensile failure for (a) ductile and (b) brittle shales for a drift spacing extended to 100 m.

5. EBS DESIGN WITH CONCENTRIC CANISTER LOCATION

The design for the EBS applied in Rutqvist (2019) and in the previous sections of the report with large-scale canisters placed on the drift floor were originally proposed by Hardin et al. (2013; 2014) for backfilled or open tunnel design. An alternative design investigated in this section is to use the Swiss concept of the emplacement in backfilled tunnels. According to the Swiss concept, the waste canister is placed in the center of the of the emplacement tunnel on a pedestal of highly compacted bentonite blocks and the rest of the tunnel is then filled with granular bentonite. The Swiss concept is for waste canisters containing 4 PWR elements; a canister is about 1 m in diameter and an emplacement tunnel is 3 m in diameter. Upscaling this concept to twice the diameter for large-scale DPCs (2 m in diameter) and a 6 m in diameter emplacement tunnel is shown in Figure 5-1. Possible engineering issues with emplacement of such large and heavy waste canisters are not investigated in this report. Here, the focus is on the thermal management and potential geomechanical issues for applying this concept in various host rocks.

As noted previously, the host rock THM response, including thermal pressurization and the host rock stress changes are not impacted by the EBS design. Thus, in order to keep the host rock THM responses at a manageable level, the 100 m drift spacing is enacted for simulations. Other thermal management key responses are impacted by the EBS design, including the peak temperature in the buffer and wall rock, and possibly the resaturation of the bentonite buffer.

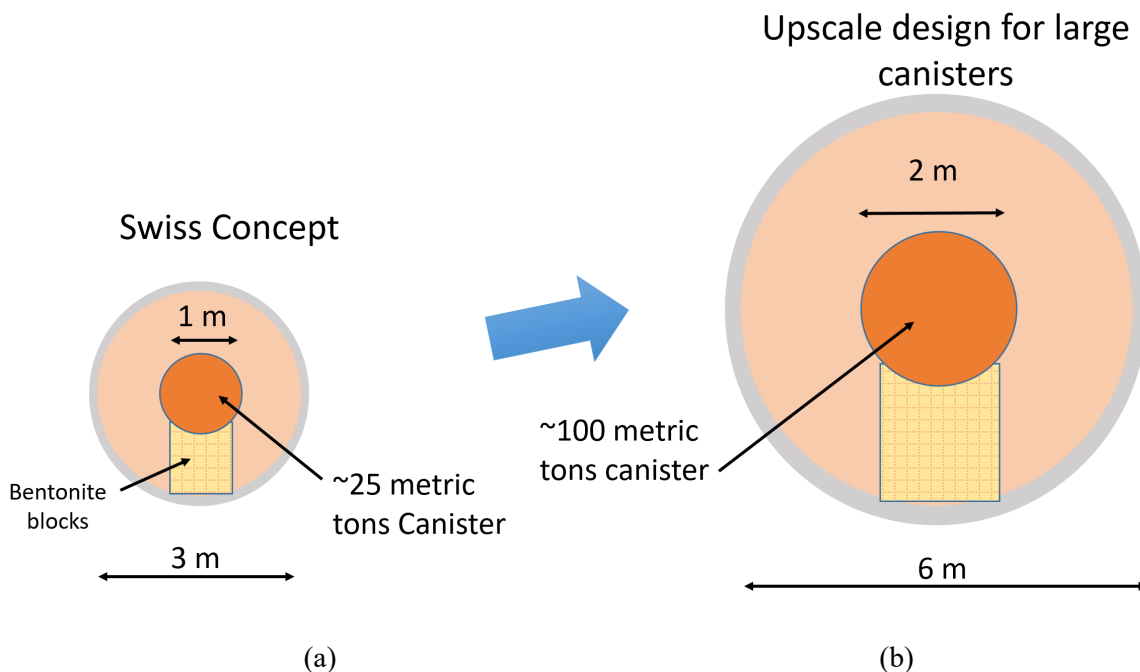


Figure 5-1. The Swiss concept of an emplacement tunnel with bentonite backfill and the canister placed on a pedestal of bentonite blocks (a), and an upscale version (b) that could potentially be applied for large scale canisters.

5.1 24-PWR DPCs 100YOoR and High Thermal Conduction Bentonite Properties

The results for 24-PWR DPCs emplaced at 100YOoR are shown in Figures 5-2 through 5-4 for the design with concentric canister emplacement. Here, the three different options of bentonite materials are considered according to the options studied in Rutqvist (2019). It is demonstrated in Figure 5-2 that the use of a bentonite buffer material that is engineered for high thermal conductivity can substantially reduce the peak temperature at the inner parts of the buffer. Here, the temperature is reduced to well below 100°C. The graphene oxide mix provide a very high thermal conductivity compared to the host rock, and it practically eliminated the thermal gradient across the buffer. The graphite option that maybe more economical is also effective in reducing the peak temperature of the buffer. However, as discussed previously, the temperature in host rock is not significantly impacted by the thermal conductivity or the exact design of the EBS, but is strongly dependent on thermal conductivity of the host rock and the spacing of the emplacement tunnels. In this case, the thermal pressurization and fluid pressure evolution are similar to those of the floor emplacement option as shown in Figure 4-6. It is shown in Figure 5-4 that the fluid pressure would not exceed the lithostatic stress and thus the possibility of hydraulic fracturing would be avoided.

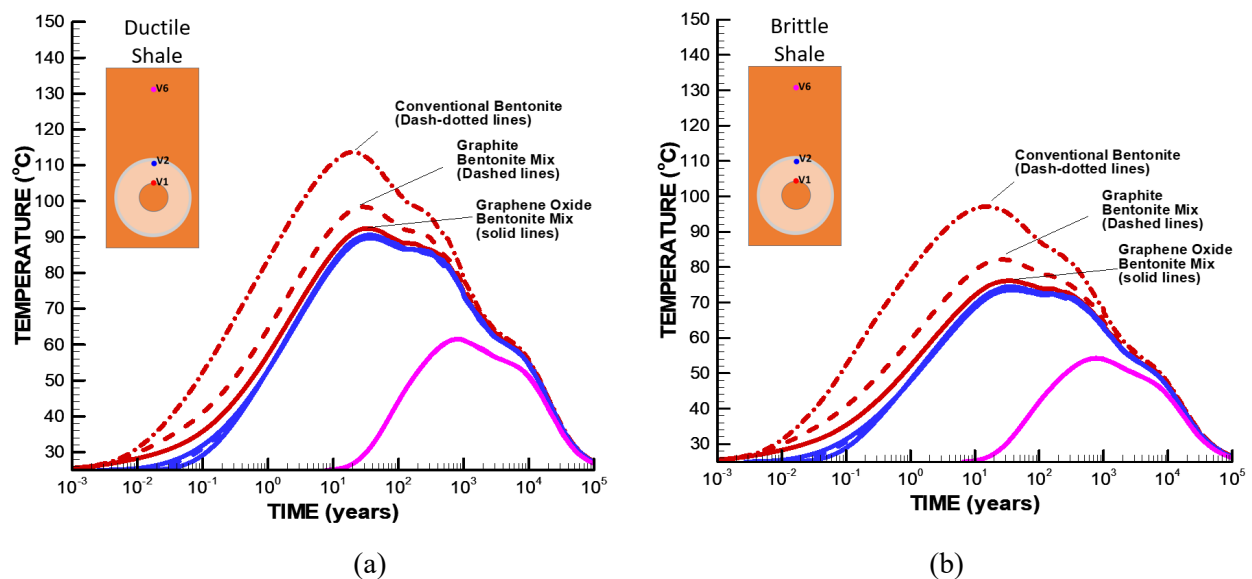


Figure 5-2. Results of simulations of the temperature evolution for (a) ductile and (b) brittle shales for concentric canister emplacement and a 100 m drift spacing.

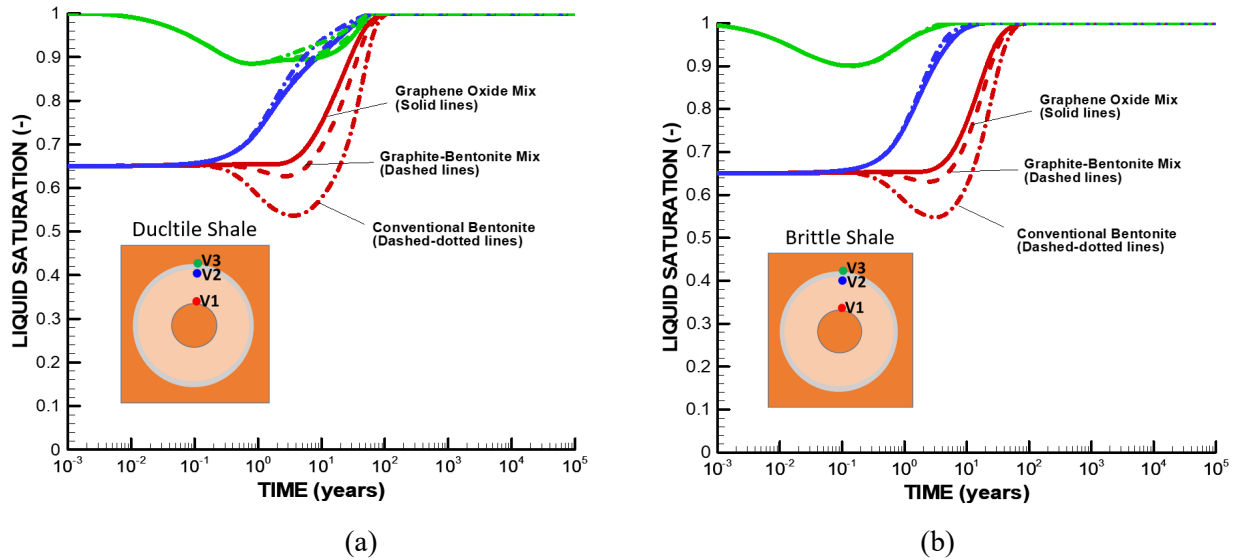


Figure 5-3. Results of simulations of the saturation evolution for (a) ductile and (b) brittle shales for concentric canister emplacement and a 100 m drift spacing.

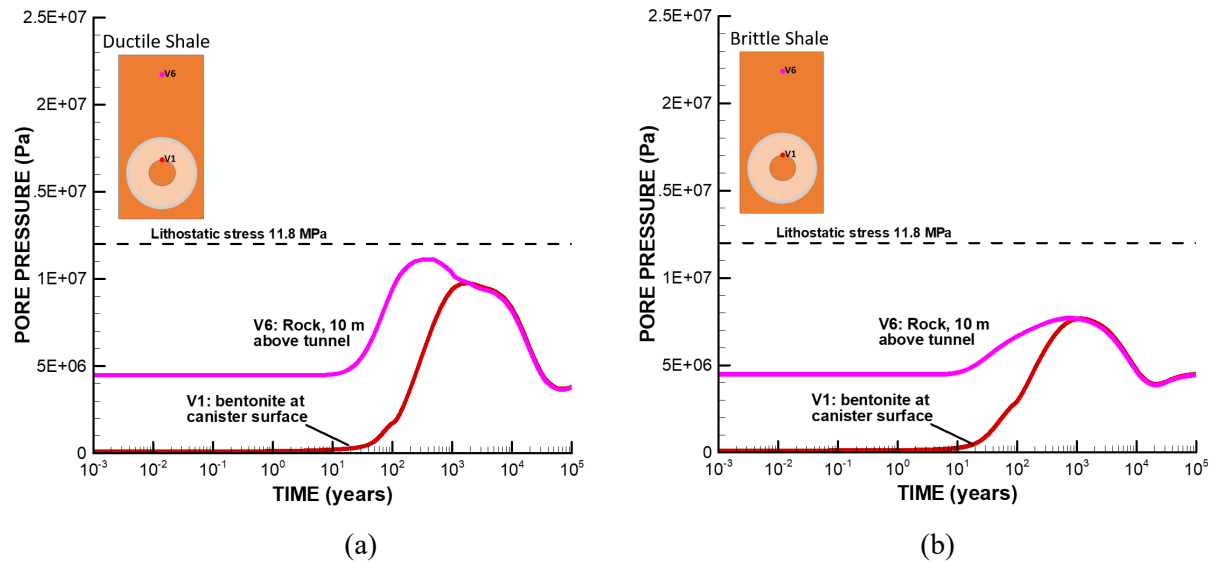


Figure 5-4. Results of simulations of the pressure evolution for (a) ductile and (b) brittle shales for concentric canister emplacement and a 100 m drift spacing.

5.2 37-PWR DPCs 100YOoR and Increased Drift Spacing

The 37-PWR DPCs emplaced after 100YOoR provide the highest heat load among the options listed in Table 2-3. The initial decay heat is large and will cause very high temperature at the inner parts of the buffer, if conventional bentonite is used. Figures 5-5 and 5-6 show temperature and pressure evolution for such a high decay heat. To limit the peak temperature at the inner parts of the buffer, a thermally engineered bentonite is considered with the properties of bentonite mixed with graphene oxide. The peak temperature goes up to 180°C in the case of ductile shale, and it would be less than 150°C for the case of brittle shale.

As mentioned, the brittle shale has higher thermal conductivity, and therefore the peak temperature is lower than in the case of ductile shale.

For the case of 37-PWR-100YoOR, the temperature in host rock increases substantially. For a 100 m drift spacing, the peak temperature in the host rock is around 80°C to 90°C for the two types of shale rocks. This causes strong thermal pressurization, especially in the case of ductile shale properties. Indeed, in the case of ductile shale, the fluid pressure exceeds the lithostatic stress by almost 10 MPa, potentially causing hydraulic fracturing. Results of simulations for 150 m and 200 m drift spacing show that the thermal pressurization can be reduced by increasing the drift spacing, but still for the 200 m drift spacing the thermally induced pressure exceeds the lithostatic stress in the case of a ductile shale. In the case of brittle shale, the fluid pressure does not exceed the lithostatic stress for a drift spacing of 100 m or more.

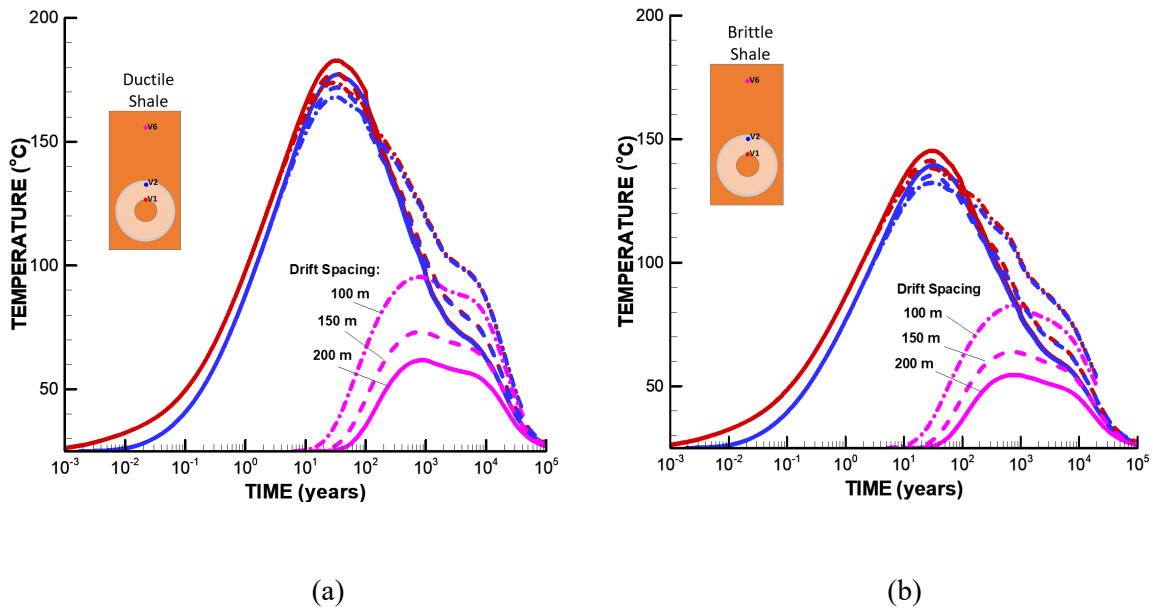


Figure 5-5. Results of simulations of the pressure evolution for (a) ductile and (b) brittle shales for concentric canister emplacement and a 100 m drift spacing.

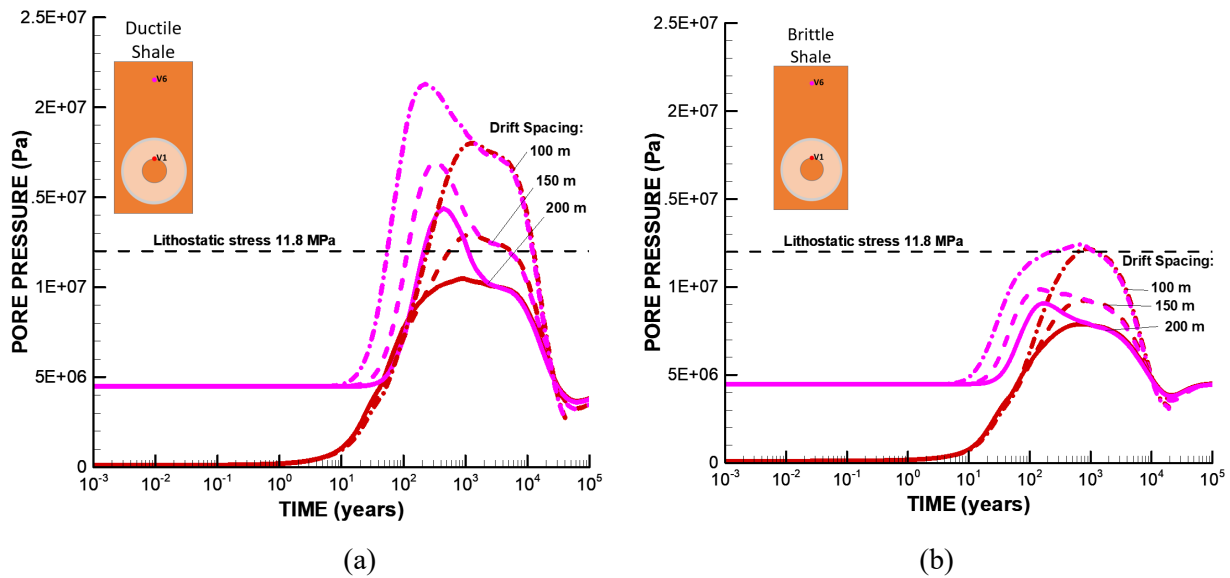


Figure 5-6. Results of simulations of the pressure evolution for (a) ductile and (b) brittle shales for concentric canister emplacement and a 100 m drift spacing.

This page is intentionally left blank.

6. SUMMARY OF FY20 PROGRESS AND FUTURE WORK

In FY19, a new research activity was initiated to provide a performance assessment of impacts of direct disposal of commercial spent nuclear fuel (SNF) in dual-purpose canisters (DPCs). The FY19 work highlighted the importance of coupled THM processes for high-temperature systems, where damage could be caused around the waste emplacement tunnels and the host rock, if the systems are not properly designed (Rutqvist, 2020). In FY20, LBNL has continued this activity by extending the assessment and designing with considering various host rock environments and rock types. Three-dimensional simulations were used for detailed prediction of the temperature evolution near the waste package, while two-dimensional simulations were employed for faster scoping simulations of various thermally induced coupled THM processes and geotechnical issues.

The results of investigations presented in this report highlight the difference in the THM behavior for ductile versus brittle shale host rocks. In case of ductile shale, the low thermal conductivity and low permeability lead to substantial thermal pressurization, which needs to be considered in the thermal management and design of a repository. In the case of brittle shale, the potential for thermal-mechanical damage to the excavation as well as the potential for shear activation of existing fractures in the host rock are issues of concern. Considering these different characteristics, repository design parameters can be used for thermal management, considering temperature limits to the EBS and host rock.

The simulation results demonstrated how temperature in the EBS could be reduced to acceptable levels considering an EBS design with a buffer engineered for high heat conduction and a large diameter emplacement tunnel. This was shown even for the highest decay heat of 37-PWRs canisters and for ductile shale host rock of the lowest thermal conductivity. The analysis further shows that the relatively modest temperature increases in the host rock can be a limiting factor as it can induce significant thermal pressurization, which combined with increasing repository shear stress can potentially cause damage to the host rock in the form of hydraulic fracturing and fracture shear activation. Temperature in the host rock can be managed by increasing the spacing between individual emplacement tunnels.

For the rest of FY20, other repository design options and host rocks will be considered, such as direct disposal of DPCs in salt host rock, which might be most suitable because of its high thermal conductivity and accelerated creep closure under conditions of elevated temperature. On the other hand, the heavy canisters might sink because of creep deformations that could be accelerated due to high temperature. These geotechnical issues will be further investigated to obtain the information needed for the design of direct disposal of DPCs in various host rocks.

This page is intentionally left blank.

7. ACKNOWLEDGEMENTS

This work was supported by the Spent Fuel and Waste Science and Technology Campaign, Office of Nuclear Energy, of the U.S. Department of Energy under Contract Number DE-AC02-05CH11231 with Lawrence Berkeley National Laboratory.

This page is intentionally left blank.

8. REFERENCES

- Alonso, E.E., et al. (2005) The FEBEX Benchmark test. Case Definition and comparison of modelling approaches. *Int. J. Rock Mech. & Min. Sci.* 42, 611–638.
- Carter, J., Luptak, A., Gastelum, J., Stockman, C. and Miller, A. (2013) Fuel Cycle Potential Waste Inventory for Disposition. FCR&D-USED-2010-000031 Rev. 6. U.S. Department of Energy, Used Fuel Disposition R&D Campaign.
- Chen, Y.G., Liu, X.M., Mu, X., Ye, W.M., Cui, Y.J., Chen, B., and Wu, D.B. (2018) Thermal conductivity of compacted GO-GMZ bentonite used as buffer material for a high-level Radioactive waste repository. *Advances in Civil Engineering*, 2018, Article ID 9530813, <https://doi.org/10.1155/2018/9530813>.
- Dobson, P., and Houseworth, J. (2014) Inventory of Shale Formations in the US, Including Geologic, Geochemical, Hydrological, Mechanical, and Thermal Characteristics. Prepared for U.S. Department of Energy, Used Fuel Disposition Campaign, FCRD-UFD-2014-000512, Lawrence Berkeley National Laboratory.
- Gens, A., Sanchez, M., Guimaraes, L.D.N., Alonso, E.E., Lloret, A., Olivella, S., Villar, M.V., and Huertas, F. (2009) A full-scale in situ heating test for high-level nuclear waste disposal: observations, analysis and interpretation. *Geotechnique*. 59, 377-399.
- Hardin, E.L., Clayton, D.J., Howard, R.L., Scaglione, J.M., Pierce, E., Banerjee, K., Voegelé, M.D., Greenberg, H.R., Wen, J., Buscheck, T.A., Carter, J.T., Severynse, T., and Nutt, W.M (2013) Preliminary Report on Dual-Purpose Canister Disposal Alternatives (FY13) FCRD-UFD-2013-000171 Rev. 1. U.S. Department of Energy, Office of Used Nuclear Fuel Disposition.
- Hardin, E, Bryan, C., Ilgen, A., Kalinina, E., Banerjee, K., Clarity, J., Howard, R., Jubin, R., Scaglione, J., Perry, F., Zheng, L., Rutqvist, J., Birkholzer, J., Greenberg, H., Carter, J., and Severynse, T. (2014) Investigations of Dual-Purpose Canister Direct Disposal Feasibility (FY14). FCRD-UFD-2014-000069 Rev. 0. U.S. Department of Energy, Office of Used Nuclear Fuel Disposition.
- Hardin, E., Price, L., Kalinina, E., Hadgu, T., Ilgen, A., Bryan, C., Scaglione, J., Banerjee, K., Clarity, J., Jubin, R., Sobes, V., Howard, R., Carter, J., Severynse, T., and Perry, F. (2015) Summary of Investigations on Technical Feasibility of Direct Disposal of Dual-Purpose Canisters. FCRD-UFD-2015-000129 Rev. 0. U.S. Department of Energy, Office of Used Nuclear Fuel Disposition.
- Perry, F.V., Kelley, R.E. Dobson, P.F., Houseworth, J.E. (2014) Regional Geology: A GIS Database for Alternative Host Rocks and Potential Siting Guidelines. LA-UR-14-20368, FCRD-UFD-2014-000068. Los Alamos National Laboratory, Los Alamos, New Mexico
- Posiva S.K.B. (2017) Safety functions, performance targets and technical design requirements for a KBS-3V repository. Posiva SKB Report 02, January 2017.
- Rutqvist, J. (2019) Geotechnical and performance assessment impacts of DPC disposal in various host rock environments. Prepared for U.S. Department of Energy, Spent Fuel and Waste Disposition, LBNL-2001220, Lawrence Berkeley National Laboratory (2019).
- Rutqvist, J. (2020) Thermal Management Associated with Geologic Disposal of Large Spent Nuclear Fuel Canisters in Tunnels with Thermally Engineered Backfill. *Tunnelling and Underground Space Technology*. 102, 103454. <https://doi.org/10.1016/j.tust.2020.103454>.

- Rutqvist, J., Ijiri, Y., and Yamamoto, H. (2011) Implementation of the Barcelona Basic Model into TOUGH-FLAC for simulations of the geomechanical behavior of unsaturated soils. *Computers & Geosciences*, 37, 751–762.
- Rutqvist, J., Zheng, L., Chen, F., Liu, H.-H., and Birkholzer, J. (2014) Modeling of Coupled Thermo-Hydro-Mechanical Processes with Links to Geochemistry Associated with Bentonite-Backfilled Repository Tunnels in Clay Formations. *Rock Mechanics and Rock Engineering*, 47, 167–186.
- Rutqvist, J., Kim, K., Xu, H., Guglielmi, Y., and Birkholzer, J. (2018) Investigation of Coupled Processes in Argillite Rock: FY18 Progress. Prepared for U.S. Department of Energy, Spent Fuel and Waste Disposition, LBNL-2001168, Lawrence Berkeley National Laboratory.
- Rutqvist, J., Guglielmi, Y., Kim, K., Xu, H., Deng, H., Li, P., Hu, M., Steefel, C., Gilbert, B., Rinaldi, A., Nico, P., Borglin, S., Fox, P., and Birkholzer, J. (2019) Investigation of coupled processes in argillite rock: FY19 progress. Prepared for U.S. Department of Energy, Spent Fuel and Waste Disposition, LBNL-2001202, Lawrence Berkeley National Laboratory.
- Sevougian, S.D., Stein, E.R., LaForce, T., Perry, F.V., Nole, M., and Chang, K.W. (2019) GDSA Repository Systems Analysis FY19 Update, SAND2019-11942R, Sandia National Laboratories, Albuquerque, NM.